Journal of King Saud University – Science (2018) 30, 301–310

King Saud University
Journal of King Saud University – Science
www.ksu.edu.sa
www.sciencedirect.com

Dispersion study of SH-wave propagation in an irregular magneto-elastic anisotropic crustal layer over an irregular heterogeneous half-space

Parvez Alam *, **Santimoy Kundu, Shishir Gupta**

Department of Applied Mathematics, Indian Institute of Technology (Indian School of Mines), Dhanbad 826004, Jharkhand, India

Received 28 August 2016; accepted 27 November 2016
Available online 7 December 2016

KEYWORDS

SH-wave;
Maxwell's;
Magneto-elastic;
Heterogeneity;
Corrugation;
Undulatory

Abstract This study investigates the effect of various parameters on the propagation of seismic SH-waves in a magneto-elastic anisotropic crustal layer with corrugated boundary surfaces, lying over a heterogeneous half-space. The shear elastic modulus and mass density of half-space are the exponential functions of depth. Inclusion of the concept of corrugated irregularity with magneto-elasticity in the anisotropic (Monoclinic) medium and heterogeneity in the half-space medium brings a novelty to the existing literature related to the study of SH-wave. The expression of general dispersion relation has been established in closed form by using suitable boundary conditions. The effects of magneto-elastic coupling, heterogeneity, corrugation, undulatory and position parameters on the phase velocity of SH-wave have been computed numerically and demonstrated graphically. Moreover, different cases of free and common surface corrugations are studied which serve as a focal theme of the study.

1. Introduction

Regulation of seismic waves like propagation, reflection, transmission and refraction through an elastic layered media (coupled with different fields) is totally controlled by the properties and divergent irregular contact surfaces of the layered media. The study of seismic waves and their characteristics is often carried out to identify the structure and dynamics of the Earth's interior as well as to detect the epicentre of earthquakes. The analysis of seismic wave propagation in some complex media is also helpful in the exploration of natural resources buried inside the Earth's surface, e.g., oils, gases, minerals, crystals, metals and other useful hydrocarbons. It infers lot of information about the velocity of the wave, inward peculiarities of the media and forms the core tool of geophysical and earthquake sciences.

The magnetic and elastic properties of magneto-elastic materials depend on each other. The Earth's crust is made of the great diversity of igneous, metamorphic and sedimentary rocks. These rocks are capable to generate magnetic field due to the presence of some ferromagnetic minerals like iron, nickel,

* Corresponding author.
E-mail addresses: alamparvez.amu@gmail.com (P. Alam), kundu_santi@yahoo.co.in (S. Kundu), shishir_ism@yahoo.com (S. Gupta).
Peer review under responsibility of King Saud University.

ELSEVIER Production and hosting by Elsevier

http://dx.doi.org/10.1016/j.jksus.2016.11.007

cobalt, etc. Hence, these rocks can be considered as the magneto-elastic body. The investigation into the SH-wave propagation in magneto-elastic bodies is quite important for the development of fundamental work on the mechanics of a magnetic body. Moreover, it may be used in various areas of science, engineering technology such as seismology, defectoscopy, geophysics, astrophysics and geo-tectonics. Keeping in view the significance of seismic wave propagation in magneto-elastic bodies, the considerable amount of investigations is carried out by several researchers. Notable among them are Abd-Alla et al. (2016), Said (2016), Majhi et al. (2016), Calas et al. (2008), Othman and Song (2006), Chattopadhyay and Singh (2014), Song et al. (2006), Abo-Dahab et al. (2015), Singh et al. (2016a) and Mahmoud (2016). Matinfar et al. (2015) observed the interaction of electromagnetic wave with electron using the variational iteration method.

It is well-known fact that the interface between any two adjacent layers of the Earth is very complicated and irregular in nature. These irregular interfaces may be in the shape of corrugation (undulated), rectangular, parabolic or much complicated and work as a catalyst in affecting the propagation behaviour of SH-waves. Some notable references related to the study of wave phenomena in/at irregular boundary surfaces are Vishwakarma and Xu (2016a), Singh and Lakshman (2016), Kundu and his co-workers (Kundu et al., 2014, 2016a), Singh et al. (2016b), Tomar and Kaur (2007) and Chatterjee et al. (2015).

The subject of wave propagation in a heterogeneous elastic medium is of great interest since long because of continuous change in the elastic properties of the material. These studies were recorded in several treatises including Birch (1952) and Bullen (1940). Subsequently, Vishwakarma and Xu (2016b), Daros (2013), Zhou et al. (2014), Sahu et al. (2014) and Kundu et al. (2016b) discussed for seismic waves in various types of heterogeneous media.

The present study investigates the affected behaviour of horizontally polarized shear wave (i.e. SH-wave) propagation in an anisotropic crustal layer of finite thickness, lying over a heterogeneous half-space. The boundary surfaces of considered structure are corrugated irregular. The crustal anisotropic layer has been regarded as a perfect conductor. The shear elastic modulus and mass density of the half-space have been considered in terms of the exponential function of depth i.e. $\mu_2 = \mu_0 e^{az}$ and $\rho_2 = \rho_0 e^{bz}$, where a and b are heterogeneous parameters. The effects of magneto-elastic coupling, upper free surface corrugation, common surface corrugation, heterogeneities and some geometrical parameters (undulatory and position) on the phase velocity of SH-wave against wave number have been shown by several graphs. This investigation for the propagation of SH-waves may be of importance when such types of waves are propagated on the Earth's surface where corrugated irregularity together with the magneto-elasticity, anisotropy and heterogeneity are present.

2. Governing equations

The Cartesian co-ordinate system has been considered in such a way that x-axis is in the direction of wave propagation and z-axis is vertically downwards. A magneto-elastic anisotropic crustal layer, $M_1 : [\lambda_1(x) - h] \leqslant z \leqslant \lambda_2(x)$ with corrugated boundary surfaces is taken in such a way that it lying over a heterogeneous half-space, $M_2 : \lambda_2(x) \leqslant z \leqslant \infty$. Here, h is the thickness of magneto-elastic anisotropic crustal layer; $\lambda_1(x)$ and $\lambda_2(x)$ are continuous and periodic functions of x independent of y, representing the corrugated boundaries of free and common surfaces as shown in Fig. 1. The appropriate Fourier series expansion of these functions can be given as (Singh, 2011; Vishwakarma and Xu, 2016a)

$$\lambda_j(x) = \sum_{n=1}^{\infty} (\lambda_n^j e^{in\alpha x} + \lambda_{-n}^j e^{-in\alpha x}), \quad j = 1, 2. \tag{1}$$

here, λ_n^j and λ_{-n}^j are the coefficients of Fourier series expansion of order n, such that

$$\lambda_{\pm n}^j = \begin{cases} \frac{a_j}{2}, & \text{for} \quad n = 1 \\ \frac{A_n^j \mp i B_n^j}{2}, & \text{for} \quad n = 2, 3, 4 \ldots \end{cases} ; j = 1, 2,$$

where A_n^j and B_n^j are the cosine and sine coefficients of Fourier series expansion of order n. In view of above expressions of λ_n^j and λ_{-n}^j, Eq. (1) leads to Tomar and Kaur (2007)

$$\lambda_j(x) = a_j \cos(\alpha x) + \sum_{n=2}^{\infty} \left[A_n^j \cos(n\alpha x) + B_n^j \sin(n\alpha x) \right], \; j = 1, 2. \tag{2}$$

The corrugated upper and common boundary surfaces of the concerned problem can be expressed by only one cosine term $\lambda_1 = a_1 \cos(\alpha x)$ and $\lambda_2 = a_2 \cos(\alpha x)$ for the wavelength $\frac{2\pi}{\alpha}$ of corrugation, where a_1 and a_2 are amplitudes of the uppermost and common corrugated surfaces and α is wave number of corrugation.

2.1. SH-wave in magneto-elastic anisotropic layer

Let $\vec{u}$ is the displacement vector field for anisotropic magneto-elastic layer whose components u_i are u_1, v_1 and w_1 in x, y and z directions respectively. Therefore, equations of motion for an anisotropic magneto-elastic layer in the presence of electromagnetic force $(\vec{J} \times \vec{B})$ that is Lorentz force are

$$\tau_{ij,j} + (\vec{J} \times \vec{B})_i = \rho_1 \frac{\partial^2 u_i}{\partial t^2} \quad i, j = 1, 2, 3, \tag{3}$$

here $(\vec{J} \times \vec{B})_i$ are the components of force $(\vec{J} \times \vec{B})$ in the i_{th} direction, $\vec{J}$ is the electric current density, $\vec{B}$ is the magnetic induction vector and ρ_1 is mass density. The stress–strain relations for the anisotropic material in xz-plane are Altenbach et al. (2004)

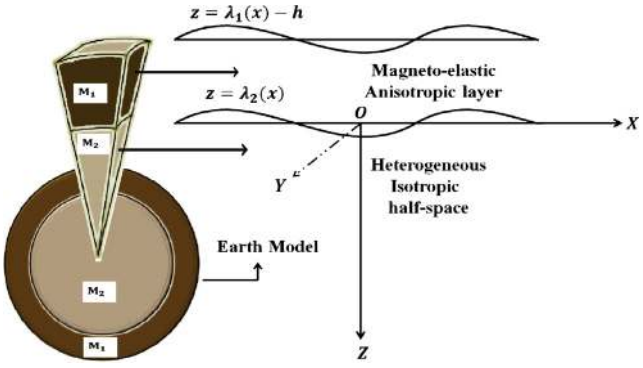

Fig. 1 Geometry of the problem,

$$\begin{aligned}
\tau_{11} &= C_{11}e_{11} + C_{12}e_{22} + C_{13}e_{33} + C_{15}e_{13},\\
\tau_{22} &= C_{12}e_{11} + C_{22}e_{22} + C_{23}e_{33} + C_{25}e_{13},\\
\tau_{33} &= C_{13}e_{11} + C_{23}e_{22} + C_{33}e_{33} + C_{35}e_{13},\\
\tau_{23} &= C_{44}e_{23} + C_{46}e_{12},\\
\tau_{13} &= C_{15}e_{11} + C_{25}e_{22} + C_{35}e_{33} + C_{55}e_{13},\\
\tau_{12} &= C_{46}e_{23} + C_{66}e_{12},
\end{aligned} \tag{4}$$

where $C_{ij} = C_{ji}(i,j = 1,2,\ldots,6)$ are elastic constants and $e_{ij} = \frac{1}{2}\left(\frac{\partial u_i}{\partial x_j} + \frac{\partial u_j}{\partial x_i}\right)$.

For the propagation of SH-wave in xz-plane

$$v_1 = v_1(x,z,t), \quad u_1 = 0 = w_1 \quad \text{and} \quad \frac{\partial}{\partial y} \equiv 0. \tag{5}$$

With the help of Eqs. (4) and (5), Eq. (3) becomes

$$\frac{\partial \tau_{12}}{\partial x} + \frac{\partial \tau_{23}}{\partial z} + \left(\vec{J} \times \vec{B}\right)_2 = \rho_1 \frac{\partial^2 v_1}{\partial t^2}, \tag{6}$$

where, $\tau_{23} = \left(C_{44}\frac{\partial v_1}{\partial z} + C_{46}\frac{\partial v_1}{\partial x}\right)$ and $\tau_{12} = \left(C_{46}\frac{\partial v_1}{\partial z} + C_{66}\frac{\partial v_1}{\partial x}\right)$.

The well known Maxwell's equations governing the electromagnetic field are Chattopadhyay and Singh (2014)

$$\vec{\nabla}\cdot\vec{B} = 0, \quad \vec{\nabla}\times\vec{E} = -\frac{\partial \vec{B}}{\partial t}, \quad \vec{\nabla}\times\vec{H} = \vec{J}, \tag{7}$$

with

$$\vec{B} = \mu_e\vec{H}, \quad \vec{J} = \sigma\left(\vec{E} + \frac{\partial \vec{u}}{\partial t}\times\vec{B}\right),$$

where $\vec{E}$ is the induced electric field, magnetic field $\vec{H}$ includes both primary and induced magnetic fields, μ_e is the induced permeability and σ is the conduction coefficient.

Let $\vec{H} = (H_1, H_2, H_3)$ and $h_i = (h_1, h_2, h_3); h_i$ is the change in the magnetic field. Then, the linearized Maxwell's stress tensor $(\tau_{ij})^M$ due to the magnetic field is given by Chattopadhyay and Singh (2014)

$$(\tau_{ij})^M = \mu_e[H_ih_j + H_jh_i - H_kh_k\delta_{ij}]. \tag{8}$$

In writing the above equations, we have neglected the displacement current. Now, from Eq. (7) we get

$$\frac{\nabla^2\vec{H}}{\sigma\mu_e} = \left[\frac{\partial \vec{H}}{\partial t} - \vec{\nabla}\times\left(\frac{\partial \vec{u}}{\partial t}\times\vec{H}\right)\right]. \tag{9}$$

In component form, Eq. (9) can be written as

$$\begin{aligned}
\tfrac{\partial H_1}{\partial t} &= \tfrac{1}{\sigma\mu_e}\nabla^2 H_1,\\
\tfrac{\partial H_2}{\partial t} &= \tfrac{1}{\sigma\mu_e}\nabla^2 H_2 + \left[\tfrac{\partial}{\partial x}\left(H_1\tfrac{\partial v_1}{\partial t}\right) + \tfrac{\partial}{\partial z}\left(H_3\tfrac{\partial v_1}{\partial t}\right)\right],\\
\tfrac{\partial H_3}{\partial t} &= \tfrac{1}{\sigma\mu_e}\nabla^2 H_2.
\end{aligned} \tag{10}$$

Now for a perfectly conducting medium, i.e., when $\sigma \to \infty$, Eq. (10) becomes

$$\frac{\partial H_1}{\partial t} = 0 = \frac{\partial H_3}{\partial t} \tag{11}$$

and

$$\frac{\partial H_2}{\partial t} = \left[\frac{\partial}{\partial x}\left(H_1\frac{\partial v_1}{\partial t}\right) + \frac{\partial}{\partial z}\left(H_3\frac{\partial v_1}{\partial t}\right)\right]. \tag{12}$$

Thus, we conclude from Eq. (11) that there is no perturbation in H_1 and H_3, but Eq. (12) shows there may be perturbation in H_2. Therefore, taking small perturbation h_2 (say) in H_2, we have

$$\begin{aligned}
H_1 &= H_{01},\\
H_2 &= H_{02} + h_2,\\
H_3 &= H_{03},
\end{aligned} \tag{13}$$

where (H_{01}, H_{02}, H_{03}) are the components of initial magnetic field $\vec{H}_0$ and initial value of h_2 should be zero.

We can write $\vec{H} = (H_0\cos\Phi, 0, H_0\sin\Phi)$, where $H_0 = |\vec{H}_0|$ and Φ is the angle at which the wave crosses the magnetic field. Thus, we have

$$\vec{H} = (H_0\cos\Phi, h_2, H_0\sin\Phi). \tag{14}$$

Using Eq. (14) in Eq. (12), we obtain

$$\frac{\partial h_2}{\partial t} = \frac{\partial}{\partial t}\left[H_0\cos\Phi\frac{\partial v_1}{\partial x} + H_0\sin\Phi\frac{\partial v_1}{\partial z}\right]. \tag{15}$$

Integrating Eq. (15) with respect to t, we get

$$h_2 = H_0\left[\cos\Phi\frac{\partial v_1}{\partial x} + \sin\Phi\frac{\partial v_1}{\partial z}\right]. \tag{16}$$

With the help of Eq. (7), we have

$$\vec{J}\times\vec{B} = \mu_e[(\vec{H}\cdot\vec{\nabla})\vec{H} - \frac{1}{2}\vec{\nabla}H^2]. \tag{17}$$

In view of Eqs. (6) and (17) with the values of τ_{12} and τ_{23}, we obtain the equation of motion for the propagation of SH-wave in anisotropic magneto-elastic medium as

$$M_{66}\frac{\partial^2 v_1}{\partial x^2} + 2M_{46}\frac{\partial^2 v_1}{\partial x\partial z} + M_{44}\frac{\partial^2 v_1}{\partial z^2} = \rho_1\frac{\partial^2 v_1}{\partial t^2}, \tag{18}$$

where $M_{66} = C_{44}\left(\frac{C_{66}}{C_{44}} + m_H\cos^2\Phi\right)$, $M_{46} = C_{44}\left(\frac{C_{46}}{C_{44}} + m_H\sin\Phi\cos\Phi\right)$, $M_{44} = C_{44}\left(1 + m_H\sin^2\Phi\right)$ and $m_H = \frac{\mu_e H_0^2}{C_{44}}$ is the magneto-elastic coupling parameter.

Let us take a harmonic solution of Eq. (18) as $v_1 = V_1(z)e^{ik(x-ct)}$ and substituting in Eq. (18), we get

$$\frac{d^2V_1(z)}{dz^2} + \zeta_1\frac{dV_1(z)}{dz} + \zeta_2 V_1(z) = 0, \tag{19}$$

where $\zeta_1 = 2ik\frac{M_{46}}{M_{44}}, \zeta_2 = k^2\left(\frac{c^2}{c_1^2} - \frac{M_{66}}{M_{44}}\right), c_1 = \sqrt{\frac{M_{44}}{\rho_1}}$ and angular frequency $\omega = kc; k$ is the wave number and c is the phase velocity of SH-wave.

The solution of Eq. (19) is obtained as

$$v_1(z) = e^{-\frac{\zeta_1}{2}z}(A\cos pz + B\sin pz)e^{ik(x-ct)}, \tag{20}$$

where, A and B are arbitrary constants and $p = \frac{\sqrt{4\zeta_2 - \zeta_1^2}}{2}$.

2.2. SH-wave in heterogeneous half-space

We have considered following transformations for the shear elastic modulus μ_2 and mass density ρ_2 of the half-space

$$\mu_2 = \mu_0 e^{az} \quad \text{and} \quad \rho_2 = \rho_0 e^{bz}, \tag{21}$$

where, a and b are small positive real heterogeneous constants having dimensions L^{-1}.

Let u_2, v_2 and w_2 are the displacement components in x, y and z directions respectively for the heterogeneous half-space. Then for the propagation of SH-wave, we have

$$v_2 = v_2(x,z,t), \quad u_2 = 0 = w_2 \quad \text{and} \quad \frac{\partial}{\partial y} \equiv 0. \tag{22}$$

The dynamical equations for the heterogeneous half-space in the absence of any body forces are given by Biot (1965)

$$\sigma_{ij,j} = \rho_2 \frac{\partial^2 v_i}{\partial t^2} \quad i,j = 1,2,3, \tag{23}$$

where $\sigma_{ij} = 2\mu_2 \varepsilon_{ij}$ are the incremental stress components, v_i represents displacement component in the i_{th} direction, i.e., u_2, v_2, w_2 and $\varepsilon_{ij} = \frac{1}{2}\left(\frac{\partial v_i}{\partial x_j} + \frac{\partial v_j}{\partial x_i}\right)$.

Using Eqs. (21) and (22) in (23), the only non-vanishing equation of motion for propagation of SH-wave in heterogeneous half-space is obtained as

$$\mu_0 e^{az} \frac{\partial^2 v_2}{\partial x^2} + a\mu_0 e^{az} \frac{\partial v_2}{\partial z} + \mu_0 e^{az} \frac{\partial^2 v_2}{\partial z^2} = \rho_0 e^{bz} \frac{\partial^2 v_2}{\partial t^2}. \tag{24}$$

Let us assume a harmonic wave solution of Eq. (24) as $v_2 = V_2(z) e^{ik(x-ct)}$ and substituting in Eq. (24), we get

$$\frac{d^2 V_2(z)}{dz^2} + a\frac{dV_2(z)}{dz} - k^2\left(1 - \frac{c^2}{c_0^2}\frac{e^{bz}}{e^{az}}\right) V_2(z) = 0, \tag{25}$$

where $c_0 = \sqrt{\frac{\mu_0}{\rho_0}}$.

For simplification of Eq. (25), we take the following substitution: $V_2(z) = \psi(z) e^{-\frac{az}{2}}$. Therefore Eq. (25) takes the form

$$\frac{d^2\psi(z)}{dz^2} + \left[\frac{k^2 c^2 (1+bz)}{c_0^2(1+az)} - k^2\left(1 + \frac{a^2}{4k^2}\right)\right]\psi(z) = 0. \tag{26}$$

Using some dimensionless quantities $\gamma = \sqrt{1 - \frac{bc^2}{ac_0^2} + \frac{a^2}{4k^2}}$ and $\phi = \frac{2k\gamma}{a}(1+az)$ in Eq. (26), then Eq. (26) reduces to

$$\frac{d^2\psi(\phi)}{d\phi^2} + \left(\frac{R}{\phi} - \frac{1}{4}\right)\psi(\phi) = 0, \tag{27}$$

where $R = \frac{kc^2(a-b)}{2\gamma c_0^2 a^2}$.

Eq. (27) is the well known Whittaker equation (Whittaker and Watson, 1990). The solution of Eq. (27) is given by

$$\psi(\phi) = DW_{R,\frac{1}{2}}(\phi) + EW_{-R,\frac{1}{2}}(-\phi), \tag{28}$$

where D and E are arbitrary constants; $W_{R,\frac{1}{2}}(\phi)$ and $W_{-R,\frac{1}{2}}(-\phi)$ are Whittaker's functions.

Now keeping in view that $\lim_{z\to\infty} V_2(z) \to 0$, *i.e.,* $\lim_{z\to\infty}\psi(\phi) \to 0$, the appropriate solution for the heterogeneous half-space may be taken as

$$v_2 = DW_{R,\frac{1}{2}}(\phi) e^{-\frac{az}{2}} e^{ik(x-ct)}. \tag{29}$$

Now using the asymptotic expansion of Whittaker's function $W_{R,\frac{1}{2}}(\phi)$ and taking its solution up to a second term, the Eq. (29) becomes

$$v_2 = D\phi e^{-\frac{\phi}{2}}\left[1 + \frac{(1-R)}{2}\phi\right] e^{-\frac{az}{2}} e^{ik(x-ct)}. \tag{30}$$

3. Boundary conditions

The boundary conditions are as follows:

3.1. Corrugated uppermost surface of the layer is traction free

$$\left[\tau_{23} + (\tau_{23})^M\right] - \lambda_1'\left[\tau_{12} + (\tau_{12})^M\right] = 0, \quad \text{at} \quad z = \lambda_1(x) - h,$$

after substituting the expressions of $\tau_{12}, \tau_{23}, (\tau_{12})^M$ and $(\tau_{23})^M$ into the above equation, we get

$$\left(M_{44}\frac{\partial v_1}{\partial z} + M_{46}\frac{\partial v_1}{\partial x}\right) - \lambda_1'\left(M_{46}\frac{\partial v_1}{\partial z} + M_{66}\frac{\partial v_1}{\partial x}\right) = 0.$$

3.2. Stresses are continuous at the common corrugated interface of the layer and half-pace

$$\left[\tau_{23} + (\tau_{23})^M\right] - \lambda_2'\left[\tau_{12} + (\tau_{12})^M\right] = \sigma_{23} - \lambda_2'\sigma_{21}, \quad \text{at} \quad z = \lambda_2(x),$$

after substituting the expressions of $\tau_{12}, \tau_{23}, (\tau_{12})^M, (\tau_{23})^M, \sigma_{12}$ and σ_{23} into the above equation, we obtain

$$\left(M_{44}\frac{\partial v_1}{\partial z} + M_{46}\frac{\partial v_1}{\partial x}\right) - \lambda_2'\left(M_{46}\frac{\partial v_1}{\partial z} + M_{66}\frac{\partial v_1}{\partial x}\right) = \mu_0 e^{az}\left(\frac{\partial v_2}{\partial z} - \lambda_2'\frac{\partial u_2}{\partial x}\right).$$

3.3. Displacements are continuous at the common corrugated interface of the layer and half-space

$$v_1 = v_2, \quad \text{at} \quad z = \lambda_2(x).$$

4. Dispersion relation

Using the solutions given in (20) and (30) into the aforementioned boundary conditions, we obtain following homogeneous algebraic system of equations for A, B and D.

$$A\left[\left(ikr_2 - r_1\frac{\zeta_1}{2}\right)\cos p(\lambda_1 - h) - r_1 p \sin p(\lambda_1 - h)\right] + B\left[\left(ikr_2 - r_1\frac{\zeta_1}{2}\right)\sin p(\lambda_1 - h) + r_1\cos p(\lambda_1 - h)\right] = 0, \tag{31}$$

$$A\left[\left(iks_2 - s_1\frac{\zeta_1}{2}\right)\cos p\lambda_2 - s_1 p\sin p\lambda_2\right] + B\left[\left(iks_2 - s_1\frac{\zeta_1}{2}\right)\sin p\lambda_2 + s_1 p\cos p\lambda_2\right] + DL = 0, \tag{32}$$

$$A\cos p\lambda_2 + B\sin p\lambda_2 + DM = 0, \tag{33}$$

where r_1, r_2, s_1, s_2, L and M are provided in Appendix A.

For such a system of simultaneous equations to have a non-trivial solution, it is necessary for the determinant of the coefficients to be zero. Hence, the below Eq. (34) must satisfy for a non-trivial solution of A, B and D

$$\tan k(h + \lambda_2 - \lambda_1)\sqrt{\frac{c^2}{c_1^2} - \frac{M_{66}}{M_{44}} + \left(\frac{M_{46}}{M_{44}}\right)^2} = \frac{N_{R_1} + iN_{R_2}}{D_R}, \tag{34}$$

where N_{R_1}, N_{R_2} and D_R are given in Appendix B.

The real part of Eq. (34) gives

$$\tan k(h+\lambda_2-\lambda_1)\sqrt{\frac{c^2}{c_1^2}-\frac{M_{66}}{M_{44}}+\left(\frac{M_{46}}{M_{44}}\right)^2}=\frac{s_1\mu_0 T\sqrt{\frac{c^2}{c_1^2}-\frac{M_{66}}{M_{44}}+\left(\frac{M_{46}}{M_{44}}\right)^2}\left[r_2^2-2r_1r_2\frac{M_{46}}{M_{44}}-r_1^2\left(\frac{c^2}{c_1^2}-\frac{M_{66}}{M_{44}}\right)\right]e^{a\lambda_2}}{\left[r_2s_2-(r_1s_2+r_2s_1)\frac{M_{46}}{M_{44}}-r_1s_1\left(\frac{c^2}{c_1^2}-\frac{M_{66}}{M_{44}}\right)+\mu_0\lambda_2'\left(r_2-r_1\frac{M_{46}}{M_{44}}\right)e^{a\lambda_2}\right]^2+\left[\mu_0 T\left(r_2-r_1\frac{M_{46}}{M_{44}}\right)e^{a\lambda_2}\right]^2}. \tag{35}$$

which is the dispersion relation for SH-wave propagation in magneto-elastic anisotropic crustal layer with corrugated boundary surfaces lying over a heterogeneous half-space.

$$\tan kh\sqrt{\frac{c^2}{c_1^2}-\frac{M_{66}}{M_{44}}+\left(\frac{M_{46}}{M_{44}}\right)^2}=\frac{r^2\mu_0\overline{T}\sqrt{\frac{c^2}{c_1^2}-\frac{M_{66}}{M_{44}}+\left(\frac{M_{46}}{M_{44}}\right)^2}\left[s\left(\frac{s}{r}-2\frac{M_{46}}{M_{44}}\right)-r\left(\frac{c^2}{c_1^2}-\frac{M_{66}}{M_{44}}\right)\right]e^{a[d\cos(\alpha x)]}}{\left[s^2-2rs\frac{M_{46}}{M_{44}}-r^2\left(\frac{c^2}{c_1^2}-\frac{M_{66}}{M_{44}}\right)-\mu_0 d\alpha\sin(\alpha x)\left(s-r\frac{M_{46}}{M_{44}}\right)e^{ad\cos(\alpha x)}\right]^2+\left[\mu_0\overline{T}\left(s-r\frac{M_{46}}{M_{44}}\right)e^{ad\cos(\alpha x)}\right]^2}, \tag{38}$$

5. Particular cases

5.1. Case I: in the absence of upper free surface corrugation

When layer is bounded by an upper free planar surface and lower common corrugated surface, i.e., $\lambda_1=0$ and $\lambda_2=a_2\cos(\alpha x)$, the dispersion relation (35) reduces to

$$\tan k[h+a_2\cos(\alpha x)]\sqrt{\frac{c^2}{c_1^2}-\frac{M_{66}}{M_{44}}+\left(\frac{M_{46}}{M_{44}}\right)^2}=\frac{\mu_0\left[\gamma+\frac{a}{2k}-\frac{a}{(1+aa_2\cos(\alpha x))}-\frac{(1-R)\gamma}{\left[1+(1-R)(1+aa_2\cos(\alpha x))\frac{\gamma k}{a}\right]}\right]e^{aa_2\cos(\alpha x)}}{\overline{s}_1\sqrt{\frac{c^2}{c_1^2}-\frac{M_{66}}{M_{44}}+\left(\frac{M_{46}}{M_{44}}\right)^2}}, \tag{36}$$

where $\overline{s}_1=[M_{44}+\alpha a_2M_{46}\sin(\alpha x)]$.

5.2. CaseII: in the absence of common surface corrugation

When layer is bounded by an upper free corrugated surface and lower common planar surface, i.e., $\lambda_1=a_1\cos(\alpha x)$ and $\lambda_2=0$, then the dispersion relation (35) reduces to

$$\tan k[h-a_1\cos(\alpha x)]\sqrt{\frac{c^2}{c_1^2}-\frac{M_{66}}{M_{44}}+\left(\frac{M_{46}}{M_{44}}\right)^2}=\frac{\mu_0M_{44}\sqrt{\frac{c^2}{c_1^2}-\frac{M_{66}}{M_{44}}+\left(\frac{M_{46}}{M_{44}}\right)^2}\left[\frac{(1-R)\gamma}{\left[1+(1-R)\frac{\gamma k}{a}\right]}+a-\left(\gamma+\frac{a}{2k}\right)\right]\left[\overline{r}_2^2-2\overline{r}_1\overline{r}_2\frac{M_{46}}{M_{44}}-\overline{r}_1^2\left(\frac{c^2}{c_1^2}-\frac{M_{66}}{M_{44}}\right)\right]}{\left[\overline{r}_1\frac{M_{46}^2}{M_{44}}+\overline{r}_1M_{44}\left(\frac{c^2}{c_1^2}-\frac{M_{66}}{M_{44}}\right)\right]^2+\left\{\mu_0\left[\frac{(1-R)\gamma}{\left[1+(1-R)\frac{\gamma k}{a}\right]}+a-\left(\gamma+\frac{a}{2k}\right)\right]\left(\overline{r}_2-\overline{r}_1\frac{M_{46}}{M_{44}}\right)\right\}^2}, \tag{37}$$

where $\overline{r}_1=[M_{44}+\alpha a_1M_{46}\sin(\alpha x)]$ and $\overline{r}_2=[M_{46}+\alpha a_1M_{66}\sin(\alpha x)]$.

5.3. Case III: for equal amplitudes of both corrugations

When the amplitude of both corrugations are equal, i.e., $a_1=a_2=d$(say) which imply $\lambda_1=\lambda_2=d\cos(\alpha x)$, then the dispersion relation (35) changes to

for values of s, r and $\overline{T}$ see Appendix C.

5.4. Case IV: for uniform isotropic media with planar boundary surfaces

When the layer (bounded by planar surfaces) is isotropic without magnetic effect and half-space is homogeneous isotropic, i.e., $\lambda_1=\lambda_2=0, m_H=0, C_{44}=C_{44}=\mu_1, C_{46}=0, a\to 0$ and $b\to 0$, then Eq. (35) reduces to

$$\tan\left[kh\sqrt{\left(\frac{c^2}{c_1^2}-1\right)}\right]=\frac{\mu_0}{\mu_1}\frac{\sqrt{1-\frac{c^2}{c_0^2}}}{\sqrt{\frac{c^2}{c_1^2}-1}}, \tag{39}$$

which is the classical Love wave equation (Love, 1920).

6. Numerical calculations and discussion

In order to study the effect of various affecting parameters on the phase velocity of SH-wave based on dispersion Eq. (35), we consider $C_{44}=94$ GPa, $C_{46}=-11$ GPa, $C_{66}=93$ GPa, $\rho_1=7450\ \mathrm{kg/m^3}$ for anisotropic magneto-elastic layer (Kumar et al., 2015) and $\mu_0=71$ GPa, $\rho_0=3321\ \mathrm{kg/m^3}$ GPa for heterogeneous half-space (Gubbins, 1990). The effect of all dimensionless parameters of considered model, namely magneto-elastic coupling parameter (m_H), heterogeneities (ah, bh), upper free surface corrugation parameter (αa_1), lower common surface corrugation parameter (αa_2), undulatory parameter (αh) and position parameter (x/h) has been evaluated numerically along with graphical representation in Figs. 2–11 for their different values. The curves of all figures

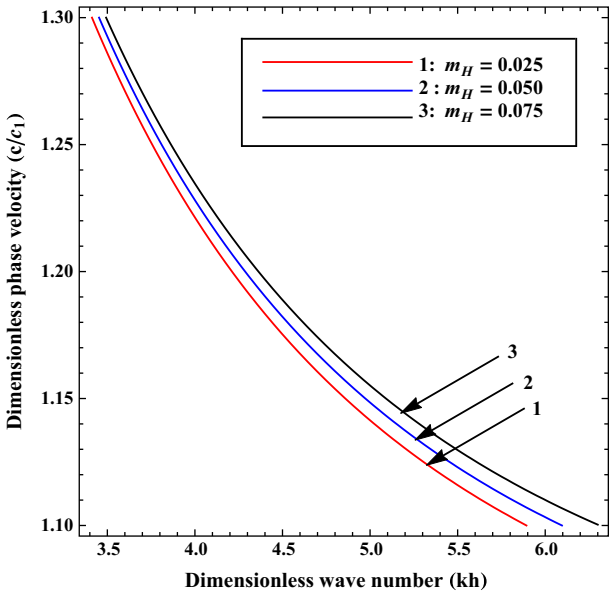

Fig. 2 Variation of phase velocity (c/c_1) against wave number (kh) for different values of m_H.

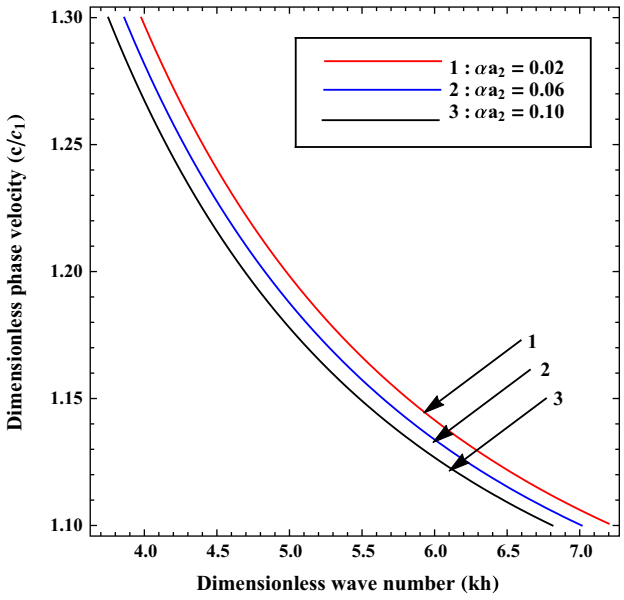

Fig. 4 Variation of phase velocity (c/c_1) against wave number (kh) for different values of αa_2.

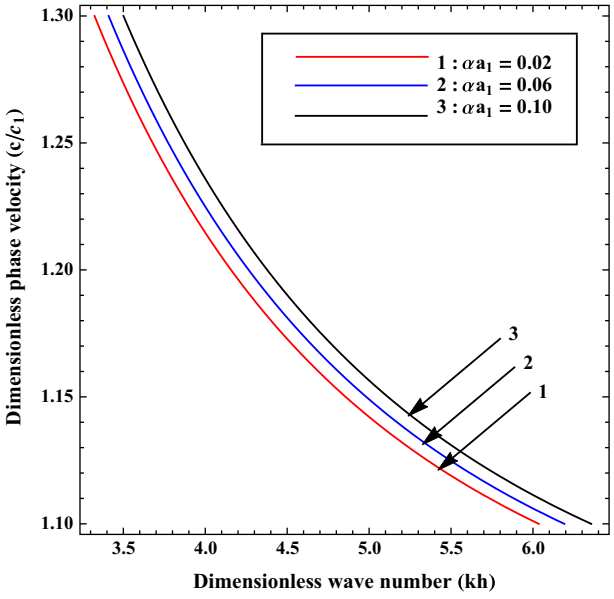

Fig. 3 Variation of phase velocity (c/c_1) against wave number (kh) for different values of αa_1.

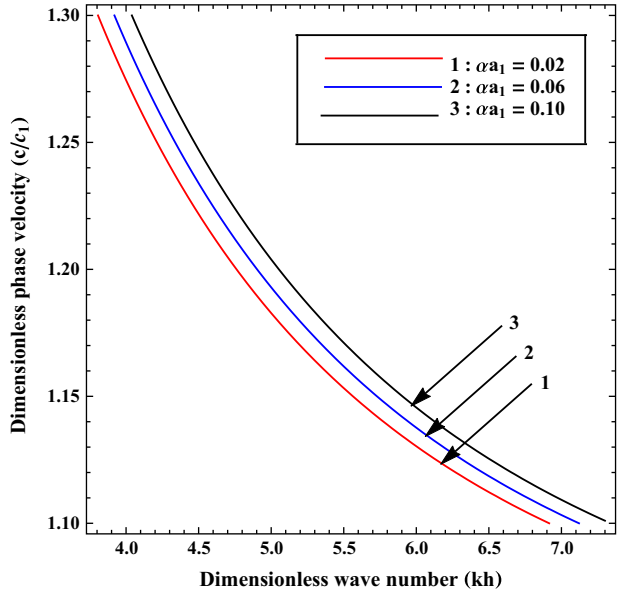

Fig. 5 Variation of phase velocity (c/c_1) against wave number (kh) for different values of αa_1, when $\alpha a_2 = 0$.

have been plotted for the dimensionless phase velocity (c/c_1) against dimensionless wave number (kh). The vertical axis in each figure represents dimensionless phase velocity (c/c_1) and the horizontal axis represents dimensionless wave number (kh). The values of parameters are given in Table 1 and angle Φ has been kept fixed to 10^o in all figures.

Fig. 2 shows the effect of magneto-elastic coupling parameter (m_H) on the dispersion curve. Value of m_H for curves 1–3 has been taken as 0.025, 0.050 and 0.075 respectively. It has been observed that as the value of m_H increases the phase velocity (c/c_1) of SH-wave also increases.

Figs. 3 and 5 describe the effect of upper corrugation parameter (αa_1) on the phase velocity of SH-wave. Fig. 5 is associated with case-I, in which common surface is planar i.e. $\alpha a_2 = 0$. In both figures, the value of (αa_1) for curves 1–3 has been taken as 0.02, 0.06 and 0.10 respectively. From these figures it has been found that, the phase velocity (c/c_1) of SH-wave increases uniformly as the value of αa_1 increases.

Figs. 4 and 6 show the influence of common corrugation parameter (αa_2) on the phase velocity of SH-wave. The curves of Fig. 6 are associated with case-II, in which upper surface of layer is planar i.e. $\alpha a_1 = 0$. Value of (αa_2) for curves 1–3 in both figures has been taken as 0.02, 0.06 and 0.10 respectively.

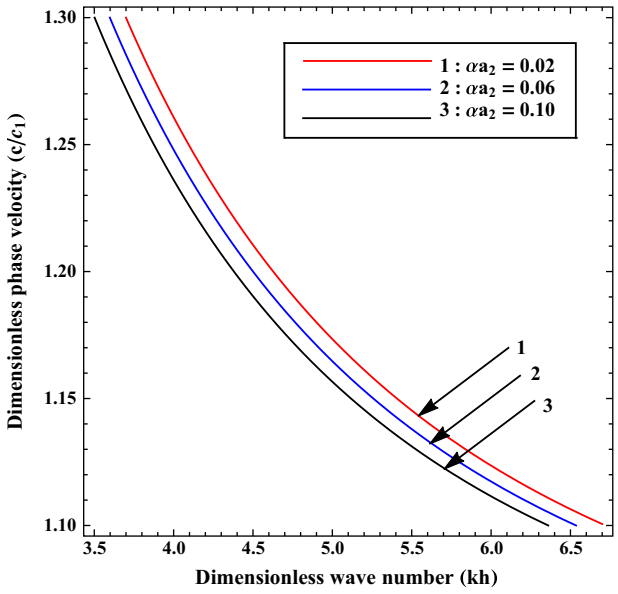

Fig. 6 Variation of phase velocity (c/c_1) against wave number (kh) for different values of αa_2, when $\alpha a_1 = 0$.

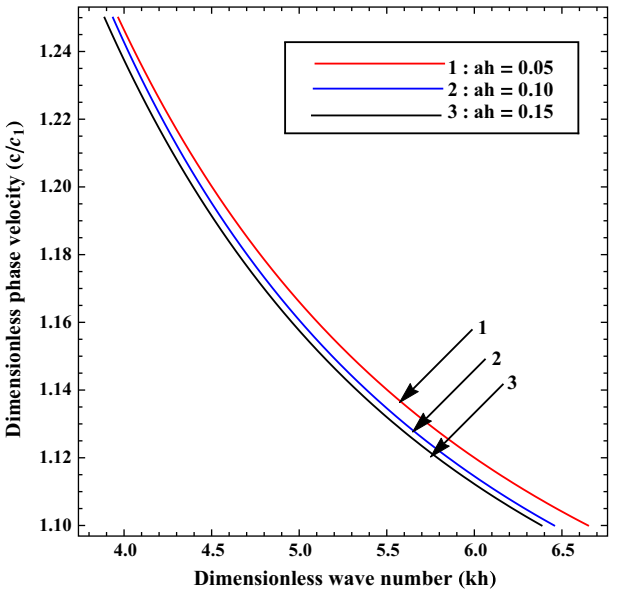

Fig. 8 Variation of phase velocity (c/c_1) against wave number (kh) for different values of ah.

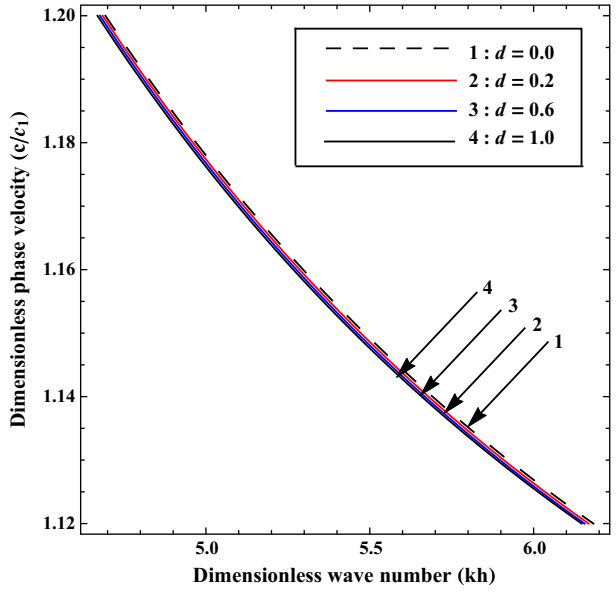

Fig. 7 Variation of phase velocity (c/c_1) against wave number (kh) for different values of $d = \alpha a_2 = \alpha a_1$.

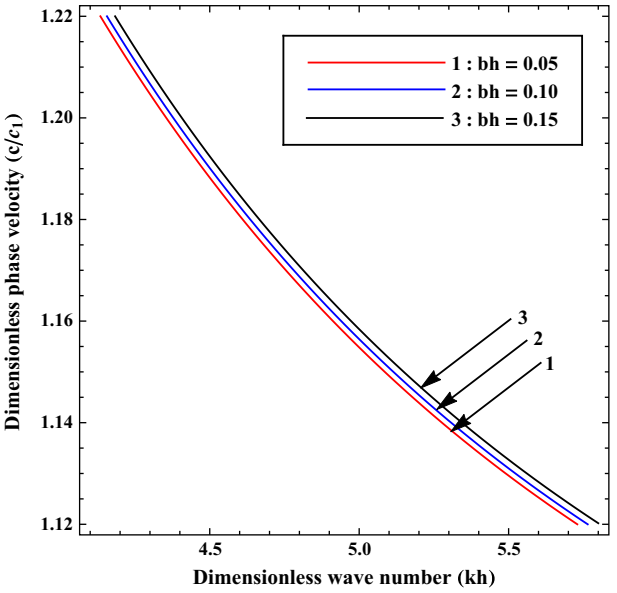

Fig. 9 Variation of phase velocity (c/c_1) against wave number (kh) for different values of bh.

It is very clear from Figs. 4 and 6 that the phase velocity (c/c_1) of SH-wave decreases uniformly with increase in αa_2.

Curves plotted in Fig. 7 are associated with case-III and show the effect of lower and upper corrugation parameters on phase velocity, when amplitudes of both cyclic corrugations are equal i.e., $\alpha a_1 = \alpha a_2 = d$ (say). Also, this figure compares the effect of planar and corrugated boundary surfaces. Value of d for curves 1–4 has been taken as 0.0, 0.4, 0.8 and 1.2 respectively. The phase velocity curve 1 represents for the uniform planar boundary surfaces of the layer, i.e., $\alpha a_1 = 0 = \alpha a_2$. It is established through the figure that the phase velocity (c/c_1) increases with an increase in d, but the increasing effect is negligible. On the other hand, when the uniform planar structure is compared with the corrugated structure, it has been found that the phase velocity of SH-wave is more in uniform planar boundary structure.

The influence of heterogeneous parameters ah and bh on the phase velocity of SH-wave is illustrated with the aid of Figs. 8 and 9. respectively. Values of ah and bh for curves 1–3 have been taken as 0.05, 0.10 and 0.15 respectively. Curve 2 of Fig. 8 shows for equal heterogeneity parameters i.e., $ah = bh = 0.1$. Meticulous observation of both figures concludes that phase velocity (c/c_1) decreases with increase in ah whereas it increases with increase in bh.

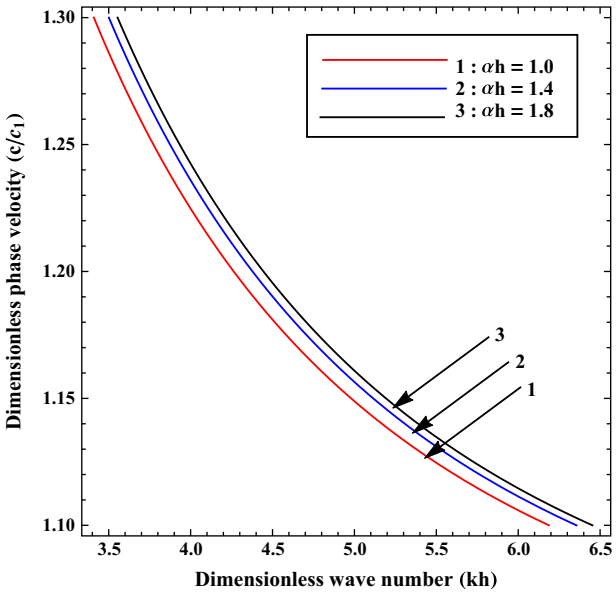

Fig. 10 Variation of phase velocity (c/c_1) against wave number (kh) for different values of αh.

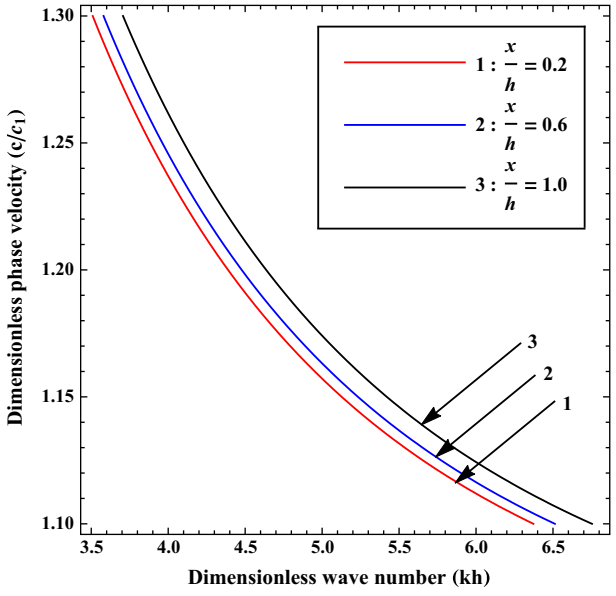

Fig. 11 Variation of phase velocity (c/c_1) against wave number (kh) for different values of x/h.

Curves plotted in Fig. 10 portray the effect of undulatory parameter (αh) on the phase velocity of SH-wave. Value of αh for curves 1–3 has been taken as 1.0, 1.4 and 1.8 respectively. It is revealed from the figure that as αh increases phase velocity (c/c_1) also increases.

Fig. 11 describes the impact of position parameter (x/h) on the phase velocity of SH-wave. Value of x/h for curves 1–3 has been taken as 0.2, 0.6 and 1.0 respectively. It has been noticed that as the value of x/h increases the phase velocity (c/c_1) of SH-wave also increases.

The results have been characterized by the fact that $c_1 < c < c_2$ (condition of SH-wave). To follow this condition, the first mode of the dispersion curve has been obtained in the approximated frequency range 3–7 of kh. So, we have considered such interval of kh in each figure. We have ignored higher values of kh, because the velocity of surface SH-waves decays with respect to depth and finally vanishes. An overview of all the figures establishes that the phase velocity (c/c_1) of SH-wave always decreases with increase of wave number (kh), which is the basic characteristic of SH-wave propagation.

7. Conclusions

The propagation of SH-wave in a magneto-elastic anisotropic crustal layer (bounded by corrugated irregular surfaces) lying over a heterogeneous half-space has been studied. Maxwell's equations have been employed to find the Lorentz force in the anisotropic layer. The non-linear differential equations are simplified by using suitable substitutions and solved using the variable separable method and Whittaker's equation. A dispersion equation has been obtained in closed form and studied for different cases of corrugations. The dispersion equation also reduces to the classical result of Love (1920) and hence validating the solutions of the problem discussed in this manuscript. The analytical findings of this work are given below.

- The magneto-elastic coupling parameter, position and undulatory parameters have favourable effect on phase velocity, that is phase velocity increases with an increase in these parameters.
- The heterogeneous parameter (ah) has inverse effect on phase velocity, whereas heterogeneous parameter (bh) has favourable effect on phase velocity. But the effect of heterogeneous parameter (ah) is significant.

Table 1 Fixed values of parameters.

Figure No.	m_H	αa_1	αa_2	ah	bh	αh	x/h
2	–	0.1	0.2	0.2	0.1	1.4	0.04
3	0.08	–	0.2	0.2	0.1	1.4	0.04
4	0.08	0.1	–	0.2	0.1	1.4	0.04
5	0.08	–	0	0.2	0.1	1.4	0.04
6	0.08	0	–	0.2	0.1	1.4	0.04
7	0.08	–	–	0.2	0.1	1.4	0.04
8	0.08	0.1	0.2	–	0.1	1.4	0.04
9	0.08	0.1	0.2	0.2	–	1.4	0.04
10	0.08	0.1	0.2	0.2	0.1	–	0.04
11	0.08	0.1	0.2	0.2	0.1	1.4	–

- Both corrugations have remarkable but unlike effect on phase velocity. Presence of upper free surface corrugation parameter increases the phase velocity, but lower common interface corrugation parameter decreases the phase velocity.
- The effects of both corrugations are found negligible when the amplitudes of both corrugations are equal. The phase velocity of wave is found more in the case of planar boundary surfaces of the layer.

It is very clear from the study that the presence of corrugated irregularities and magneto-elastic behaviour of layer have prominent effect on the propagation of SH-wave, especially for unequal amplitudes of corrugations. From the last two–three decades maximum earthquakes have occurred in the crust only and draw attention for seismologists to study the seismic waves in different kind of layered media. The results obtained in this paper give some essential information about the velocity of SH-wave propagation in Earth's crustal layer which is anisotropic (Monoclinic) and corrugated irregular with magnetic behaviour. These results may play a vital role to understand well and predict the seismic wave behaviour at continental margins, mountain roots, etc.

8. Funding

This research received no specific grant from any funding agency in the public, commercial, or not-for-profit sectors.

Appendix A.

$$r_1 = (M_{44} - \lambda_1' M_{46}),$$
$$r_2 = (M_{46} - \lambda_1' M_{66}),$$
$$s_1 = (M_{44} - \lambda_2' M_{46}),$$
$$s_2 = (M_{46} - \lambda_2' M_{66}),$$
$$L = \frac{2\gamma k\mu_0}{a} e^{-\left[\frac{\gamma k}{a}+\left(\gamma k+\frac{a}{2}\right)\lambda_2\right]}\left[1+(1-R)(1+a\lambda_2)\frac{\gamma k}{a}\right]e^{(a+\frac{\zeta_1}{2})\lambda_2} \times\left\{(1+a\lambda_2)\left[\left(\gamma k+\frac{a}{2}\right)+ik\lambda_2'\right]-a-\frac{[(1-R)(1+a\lambda_2)\gamma k]}{\left[1+(1-R)(1+a\lambda_2)\frac{\gamma k}{a}\right]}\right\},$$
$$M = -\frac{2\gamma k}{a} e^{-\left[\frac{\gamma k}{a}+\left(\gamma k+\frac{a}{2}\right)\lambda_2\right]}\left[(1+a\lambda_2)+(1-R)(1+a\lambda_2)^2\frac{\gamma k}{a}\right]e^{\frac{\zeta_1}{2}\lambda_2}.$$

Appendix B.

$$N_{R_1} = s_1\mu_0 T\sqrt{\frac{c_2^2}{c_1^2}-\frac{M_{66}}{M_{44}}+\left(\frac{M_{46}}{M_{44}}\right)^2}\left[r_2^2-2r_1r_2\frac{M_{46}}{M_{44}}-r_1^2\left(\frac{c_2^2}{c_1^2}-\frac{M_{66}}{M_{44}}\right)\right]e^{a\lambda_2},$$
$$N_{R_2} = \sqrt{\frac{c_2^2}{c_1^2}-\frac{M_{66}}{M_{44}}+\left(\frac{M_{46}}{M_{44}}\right)^2}\left\{r_1\mu_0^2T^2\left(r_1\frac{M_{46}}{M_{44}}-r_2\right)e^{2a\lambda_2} + \left[(r_2s_1-r_1s_2)+r_1\mu_0\lambda_2'e^{a\lambda_2}\right]\times\left[r_2s_2+-(r_1s_2+r_2s_1)\frac{M_{46}}{M_{44}}\right. \left.+\left(r_2-r_1\frac{M_{46}}{M_{44}}\right)\mu_0e^{a\lambda_2}\lambda_2'-r_1s_1\left(\frac{c_2^2}{c_1^2}-\frac{M_{66}}{M_{44}}\right)\right]\right\},$$
$$D_R = \left[r_2s_2-(r_1s_2+r_2s_1)\frac{M_{46}}{M_{44}}-r_1s_1\left(\frac{c_2^2}{c_1^2}-\frac{M_{66}}{M_{44}}\right)+\mu_0\lambda_2'\left(r_2-r_1\frac{M_{46}}{M_{44}}\right)e^{a\lambda_2}\right]^2 + \left[\mu_0T\left(r_2-r_1\frac{M_{46}}{M_{44}}\right)e^{a\lambda_2}\right]^2,$$
$$T = \left[\frac{(1-R)\gamma}{\left[1+(1-R)(1+a\lambda_2)\frac{\gamma k}{a}\right]}+\frac{a}{(1+a\lambda_2)}-\left(\gamma+\frac{a}{2k}\right)\right].$$

Appendix C.

$$r = [M_{44}+\alpha dM_{46}\sin(\alpha x)],$$
$$s = [M_{46}+\alpha dM_{66}\sin(\alpha x)],$$
$$\overline{T} = \left[\frac{(1-R)\gamma}{\left[1+(1-R)[1+ad\cos(\alpha x)]\frac{\gamma k}{a}\right]}+\frac{a}{[1+ad\cos(\alpha x)]}-\left(\gamma+\frac{a}{2k}\right)\right].$$

References

Abd-Alla, A.M., Abo-Dahab, S.M., Kilany, A.A., 2016. SV-waves incidence at interface between solid-liquid media under electromagnetic field and initial stress in the context of three thermoelastic theories. J. Therm. Stresses 39 (8), 960–976.

Abo-Dahab, S.M., Abd-Alla, A.M., Khan, A., 2015. Magnetism and rotation effect on surface waves in fibre-reinforced anisotropic general viscoelastic media of higher order. J. Mech. Sci. Tech. 29 (8), 3381–3394.

Altenbach, H., Altenbach, J., Kissing, W., 2004. Mechanics of Composite Structural Elements. Springer-Verlag, Berlin Heidelberg, New York.

Biot, M.A., 1965. Mechanics of Incremental Deformations. Wiley, New York.

Birch, F., 1952. Elasticity and constitution of the earth's interior. J. Geoph. Res. 57 (2), 227–286.

Bullen, K.E., 1940. The problem of the earth's density variation. Bull. Seismol. Soc. Am. 30 (3), 235–250.

Calas, H., Otero, J.A., Rodr, R., Monsivais, G., Stern, C., 2008. Dispersion relations for SH wave in magneto-electro-elastic heterostructures. Int. J. Solids Struct. 45 (20), 5356–5367.

Chatterjee, M., Dhua, S., Chattopadhyay, A., 2015. Response of moving load due to irregularity in slightly compressible, finitely deformed elastic media. Mech. Res. Commun. 66, 49–59.

Chattopadhyay, A., Singh, A.K., 2014. Propagation of a crack due to magnetoelastic shear waves in a self-reinforced medium. J. Vibr. Cont. 20 (3), 406–420.

Daros, C.H., 2013. Green's function for SH-waves in inhomogeneous anisotropic elastic solid with power-function velocity variation. Wave Motion 50 (2), 101–110.

Gubbins, D., 1990. Seismology and Plate Tectonics. Cambridge University Press, Cambridge, U.K..

Kumar, S., Pal, P.C., Majhi, S., 2015. Reflection and transmission of plane SH-waves through an anisotropic magnetoelastic layer sandwiched between two semi-infinite inhomogeneous viscoelastic half-spaces. Pure Appl. Geophy. 172 (10), 2621–2634.

Kundu, S., Manna, S., Gupta, S., 2014. Love wave dispersion in pre-stressed homogeneous medium over a porous half-space with irregular boundary surfaces. Intern. J. Solid Struct. 51 (21), 3689–3697.

Kundu, S., Kumari, A., Gupta, S., Pandit, D.K., 2016a. Effect of periodic corrugation, reinforcement, heterogeneity and initial stress on Love wave propagation. Waves Random Compl. Med. http://dx.doi.org/10.1080/17455030.2016.1168951.

Kundu, S., Alam, P., Gupta, S., Pandit, D.K., 2016b. Impacts on the propagation of SH-waves in a heterogeneous viscoelastic layer sandwiched between an anisotropic porous layer and an initially stressed isotropic half space. J. Mech. http://dx.doi.org/10.1017/jmech.2016.43.

Love, A.E.H., 1920. Mathematical Theory of Elasticity. Cambridge University Press, UK.

Mahmoud, S.R., 2016. An analytical solution for the effect of initial stress, rotation, magnetic field and a periodic loading in a thermo-viscoelastic medium with a spherical cavity. Mech. Adv. Mater. Struct. 23 (1), 1–7.

Majhi, S., Pal, P.C., Kumar, S., 2016. Reflection and transmission of plane SH-waves in an initially stressed inhomogeneous anisotropic

magnetoelastic medium. J. Seismic. http://dx.doi.org/10.1007/s10950-016-9592-6.
Matinfar, M., Mirzanezhad, S., Ghasemi, M., Salehi, M., 2015. Solving the interaction of electromagnetic wave with electron by VIM. JKSU 27, 63–70.
Othman, M.I.A., Song, Y., 2006. The effect of rotation on the reflection of magneto-thermoelastic waves under thermoelasticity without energy dissipation. Acta Mech. 184 (1–4), 189–204.
Sahu, S.A., Saroj, P.K., Dewangan, N., 2014. SH-Waves in viscoelastic heterogeneous layer over half-space with self-weight. Arch. Appl. Mech. 84, 235–245.
Said, S.M., 2016. Influence of gravity on generalized magneto-thermoelastic medium for three-phase-lag model. J. Comput. Appl. Math. 291, 142–157.
Singh, S.S., 2011. Love wave at a layer medium bounded by irregular boundary surfaces. J. Vibr. Cont. 17 (5), 789–795.
Singh, A.K., Lakshman, A., 2016. Effect of loosely bonded undulated boundary surfaces of doubly layered half-space on the propagation of torsional wave. Mech. Res. Commun. 73, 91–106.
Singh, A.K., Kumar, S., Chattopadhyay, A., 2016a. Effect of smooth moving punch in an initially stressed monoclinic magnetoelastic crystalline medium due to shear wave propagation. J. Vibr. Cont. 22 (11), 2719–2730.
Singh, A.K., Mistri, K.C., Das, A., Chattopadhyay, A., 2016b. Propagation of love-type wave in a corrugated fibre-reinforced layer. J. Mech. http://dx.doi.org/10.1017/jmech.2016.40.
Song, Y.Q., Zhang, Y.C., Xu, H.Y., Lu, B.H., 2006. Magneto-thermoviscoelastic wave propagation at the interface between two micropolar viscoelastic media. Appl. Math. comput. 176 (2), 785–802.
Tomar, S.K., Kaur, J., 2007. Shear waves at a corrugated interface between anisotropic elastic and visco-elastic solid half-spaces. J. Seismolog. 11 (3), 235–258.
Vishwakarma, S.K., Xu, R., 2016a. Rayleigh wave dispersion in an irregular sandy Earth's crust over orthotropic mantle. Appl. Math. Model. http://dx.doi.org/10.1016/j.apm.2016.05.020.
Vishwakarma, S.K., Xu, R., 2016b. Impact of quadratically varying rigidity and linearly varying density on the Rayleigh wave propagation: An analytic solution. Int. J. Solid Strut. http://dx.doi.org/10.1016/j.ijsolstr.2016.07.031.
Whittaker, E., Watson, G.N., 1990. A Course of Modern Analysis. Universal Book Stall, New Delhi.
Zhou, C., Hu, C., Ma, F., Liu, D., 2014. Elastic wave scattering and dynamic stress concentrations in exponential graded materials with two elliptic holes. Wave Motion 51 (3), 466–475.